



A combined IR and XRD study of natural well crystalline goethites (α -FeOOH)

Stephan Kaufhold¹ · Kristian Ufer¹ · Melanie Hein¹ · Niko Götze¹ · Reiner Dohrmann^{1,2}

Received: 16 March 2022 / Revised: 11 May 2022 / Accepted: 12 May 2022 / Published online: 24 June 2022
© The Author(s) 2022

Abstract Goethite (α -FeOOH) is one of the most abundant minerals on the Earth surface, occurring in temperate, tropical and equatorial climates. Fe in goethite can be substituted by many cations such as Al, Ni for instance. A large amount of research has been conducted on the effect of varying elemental compositions (mainly Al-content) on the spectral features of goethites with most of the studies based on materials synthesized with different elemental ratios. The different elemental ratios, however, may not only affect the composition of the products but also their crystallinity and/or particle size and shape. Both parameters are known to affect results of both X-ray diffraction (XRD) and infrared spectroscopy (IR). These methods are predominantly used to characterize goethites. In the present study, therefore, a significant set of natural goethites was considered in order to investigate the effect of elemental composition on XRD and IR results. The focus was on crystallised samples which had a limited chemical variability but artefacts caused by the presence of admixtures could be excluded in most cases. First of all Rietveld refinement was optimized based on varying different parameters. A fairly good correlation of Rietveld derived crystallite sizes and specific surface area determined by N₂-adsorption (SSA) was found which proves the importance of considering the crystallite size parameters for Rietveld refinement and at the same times proves the quality of it. Using IR spectroscopy yet published relations of band

position and Al-content could be confirmed despite the fact that the range of Al-contents was small. However, the band position of the Fe–O stretching, previously used as proxy for crystallinity assessment, was found to be least variable hence contradicting yet published results. Controversial results were also published for the effect of the Al-content on the position of the asymmetric FeOH stretching band at 450 cm⁻¹. The goethites investigated in the present study indicate that the crystallite size determines the band position rather than the Al-content which is at least valid for the limited range of Al-contents. The results of the present study indicate that using synthetic sample sets bears the problem that more than one parameter might show systematic differences (e.g. crystallite size in a set of chemically varied goethites). The paper, therefore, provides IR reference data based on a set of natural well crystallised goethites.

Keywords Crystallinity · Goethite · IR-spectrometry · X-ray diffraction · XRD rietveld refinement · Characterization

1 Introduction

The chemical formula for the mineral goethite is α -FeOOH. Goethites are synthetically produced and used as pigments e.g. in paints for which they were already used in ancient times (Rose 2016). Natural goethites are important in geoscience not only because they are one of the most abundant phases in soils and weathered rocks but also because of their reactive surface area and potential to immobilize heavy metals such as Cr, V, Ni, Co (amongst others). Microbial activity in soils may reduce iron and transform iron oxide phases including magnetite (Fassbinder et al. 1990) and goethite coated with natural organic

✉ Stephan Kaufhold
s.kaufhold@bgr.de

¹ Bundesanstalt für Geowissenschaften und Rohstoffe, BGR, Stilleweg 2, 30655 Hannover, Germany

² Landesamt für Bergbau, Energie und Geologie, LBEG, Stilleweg 2, 30655 Hannover, Germany

matter (Poggenburg et al. 2018). In soil environments, iron oxyhydroxides are known to stabilize organic matter (OM) under oxic conditions (e.g. Mikutta et al. 2006) preventing release of CO₂ in the atmosphere. Such iron oxyhydroxides may possibly have protected relicts of microbial communities in Martian subsurface beneath the oxidized zone (Wickramaratna et al. 2021).

Most (mineral) phases can accommodate minor amounts of trace elements in their structure (Goldschmidt 1926) leading to a certain “phase width” (range of composition of a phase without significantly affecting its crystal structure). Goethites are special among minerals because they can accommodate particularly large amounts of cations other than Fe in their lattice. The Fe of goethites can be substituted by Al, Cd, Co, Cu, Ge, Mn, Ni, Pb, Ti, V, Zn, and Sc (Krehula and Musić 2008; Manceau et al. 2000; Martin et al. 1997; Singh et al. 2002; Levard et al. 2018). Goethites also vary with respect to their particle (crystal-lite) size, crystallinity (degree of structural order), and morphology. All these variables (composition, size, morphology) may affect infrared (IR) spectra and X-ray diffraction (XRD) pattern. Natural goethites (e.g. (Norrish and Taylor 1961)) were investigated as well as synthetic ones (e.g. Ruan et al. 2002). The advantage of investigating synthetic goethites is that single parameters such as Al-content can be controlled. However, because of the smaller diameter of the Al atom the crystallinity will also be affected by increasing the Al-content. It is, therefore, difficult to fix all relevant parameters even in a series of synthetic samples. A compilation of IR data of natural and synthetic goethites is given in Table 1.

“Crystallinity”—describing the degree of structural order of a lattice—and particle size are often related and difficult to distinguish. Larger crystals commonly exhibit a higher degree of structural order which, however, is not necessarily the case. A systematic study about the effect of crystallinity on the IR data of goethites was provided by Cambier (1986a, b). He used the specific surface area (SSA) determined by nitrogen adsorption (BET specific surface area) as measure of the crystallinity. His samples varied with respect to the SSA from 13–150 m² g⁻¹ which corresponds to the range of SSA values of natural samples. High SSA values are explained both by microporosity and small particle size. In case of goethite one may suspect the existence of some ferrihydrite admixtures which would also increase the SSA (microporosity). The parameter “oxalate extractable Fe” can be used to ensure that significant ferrihydrite contents were absent. Cambier (1986a, b) showed that the position of the OH stretching bands decreased whereas the position of the OH bending bands slightly increased with increasing crystallinity. The Fe–O band at 400 cm⁻¹ was not affected by crystallinity changes. According to Sato et al. (1969) the Fe–O

stretching band at 630 cm⁻¹ is particularly useful to study goethite crystallinity.

Cambier (1986a, b) recognized that the Fe–O stretching band at 630 cm⁻¹ (approximately parallel to the a-axis) and the Fe–OH stretching band at 400 cm⁻¹ (approximately parallel to the c-axis) are affected by the particle shape. As long as the particle elongation remains parallel to the c-axis, the band at 400 cm⁻¹, however, will be unaffected.

The particle size was found to affect both the colour of the goethite and the band intensities (Scheinost et al. 1999) rather than their band positions. For soil goethites, Norrish and Taylor (1961) found that the Al-content increases with decreasing particle size. The parameters particle size and Al-content, therefore, can be related and at least in this sample set correlated with crystallinity as well. Notably, crystallinity can be understood as the size of the coherent scattering domains. A particle, on the other hand, may consist of several coherent scattering domains.

A lot of studies were conducted on the effect of Al-substitution on the IR spectra of goethites probably because the effect of isomorphic substitution on the band positions is more significant compared to crystallinity or particle morphology. Increasing Al-content generally leads to a shift of the band positions to higher values (with few exceptions). Ruan et al. (2002) state that the band shift of goethite bands caused by Al-substitution corresponds to small changes in the lattice parameters. They also found that increasing Al-substitution leads to a larger amount of non-stoichiometric hydroxyl stretching bands. Hazemann et al. (1992) based on (Thiel 1963; Schulze 1984; Schulze and Schwertmann 1984, 1987) explained the reason for the shift by the differences of the ionic radii of Al³⁺ (0.53 Å) and Fe³⁺ (0.64 Å). Isomorphic substitution hence causes “variations in unit cell parameters and structural disorders at high substitution rate”. According to Scheinost et al. (1999) the increasing mismatch of both types of octahedra (Al and Fe) leads to a maximum of Al-substitution in goethites of about 30%. Schulze (1984) showed that the unit cell parameters c and b of Al substituted goethites are well correlated with the Al-content (decrease with increasing Al content up to 30%). The a-axis in contrast was found to be variable. According to Mendelovici et al. (1979) the Fe–O band shifts up to 460 cm⁻¹ due to Al substitution causing H bond weakening. According to Jónás and Solymár (1970) and Fysch and Fredericks (1983) band shifts caused by isomorphous Al-substitution can be best observed considering bending bands (e.g. the 900 cm⁻¹ band, Fysch and Fredericks 1983).

Most studies about the effect of Al-substitution on the IR spectra of goethite provide consistent results. Controversial results, however, were found for Blanch et al. (2008) and Ruan et al. (2002). These results are marked in

Table 1 Compilation of IR data of goethites

	MIR	3140 s	1790 w	1660 w	1645 m	1340 w	900 s	800 s	680 sh	610 s	500 sh	450 m	410 s
<i>Band assignment</i>													
Verdonck et al. (1982)									In plane OH bend	FeO stretch	FeO asym stretch	Fe3-OH stretch	FeOH asym stretch
Morterra et al. (1984)		OH stretch	Overtone	Combin			In plane OH def	Out of plane OH def					
Ruan et al. (2002)						Non-stoichiometrical OH							
<i>Band positions</i>													
Blanch et al. (2008)	0 → 10 mol% Al								670 → 677	633 → 646	497 → 508	450 → 435	409 → 414
Ruan et al. (2002)	0 → 30 mol% Al	3206 → 3233					888 → 913	798 → 809		619 → 584		461 → 480	
Cambier (1986a)							892	795		630			400
Cambier (1986b)	Incr. Crystallinity	3170 → 3147					885 → 890	791 → 793		Variable			
Fysch & Fredericks (1983)	9.4% Al						901	799		632			418
Marel & Beutelspacher (1976)	Range	3100–3140			1615–1640		880–900	800	670	610	474–500	461	425–430

Table 1. According to Ruan et al. (2002), all band positions increased with increasing Al-content except for the Fe–O stretching which decreased from Al-poor goethite (619 cm^{-1}) down to 584 cm^{-1} in case of 30% Al-substitution. In contrast, Blanch et al. (2008) reported increasing band position of the Fe–O stretching from 633 cm^{-1} up to 647 cm^{-1} with increasing Al-substitution (0–10 mol%). Interestingly Blanch et al. (2008) also found one band with a decreasing band position caused by increasing Al-content. They showed that the Fe(3)–OH band position decreased from 450 down to 435 cm^{-1} with increasing Al-content while Ruan et al. (2002) showed the opposite (see Table 1). Blanch et al. (2008) suspected these differences to result either from different sample preparation, deconvolution procedure, and/or adsorbed water.

Interestingly, most studies on the effect of isomorphic substitution on the IR spectra of goethites focus on Al only. However, as explained above, many more cations can be incorporated in the goethite structure by isomorphous substitution of Fe atoms. Martin et al. (1997), Manceau et al. (2000), and Sileo et al. (2004) carried out extended X-ray absorption fine structure (EXAFS) and X-ray absorption near edge spectroscopy (XANES) considering different cations but did not provide IR data. In these studies the coordination of the different trace elements in goethites is disclosed which may help to understand the IR data of different goethites. Manceau et al. (2000), however, pointed out that in their study not all trace elements substituted Fe atoms in the goethite structure (= isomorphous substitution) of their sample. They identified “no more than ~20 % of the amounts of Mn and Co in natural goethite substitute for Fe in the structure”.

Fysch and Fredericks (1983) found that the band shifts differ for hydrothermal and low-temperature goethites. The low-T goethites showed a more pronounced band shift of the OH bending vibration at 900 cm^{-1} . Morterra et al. (1984) distinguished pigment type goethites with N_2 -BET-surface areas ranging from $10\text{--}25\text{ m}^2\text{ g}^{-1}$ from high surface microporous goethites.

Apart from shifts of the band positions also the relative intensities of the bands can vary which was explained by different orientations of the particles (Morterra et al. 1984).

Most studies conducted on the IR spectra of goethites either focused on a few samples or on a set of synthetically varied samples. Often the goethite–hematite series was studied (Ruan et al. 2002; Rochester and Topham 1979; Hakeem et al. 1986; Rabie and Balkees 1986; Kustova et al. 1992) based on heat treatment, which was not the aim of the study. The focus for sample collection was on crystallised goethites. The advantage of such samples is that low crystallised phases are largely absent and difficult to detect admixtures such as ferrihydrite and/or amorphous Fe-oxhydroxides would not affect the results. On the other

hand, the compositional variability of such crystallised goethites was thought to be lower compared to soil or laterite goethites which would lead to less significant correlations of composition and IR/XRD parameters. Principally, one can either collect a set of significantly variable goethite samples of questionable purity or focus on the more crystallised materials. Using synthetic materials bears the problem of (i) the possible existence of amorphous or low crystallised admixtures and (ii) unwanted variation of parameters other than composition in a sample set such as crystallinity and/or crystallite size. In the present study natural but apparently crystallised goethites were collected because they were considered to represent natural materials and natural variability and the expected trends can probably be extrapolated because they are based on structural effects.

The aim of the present study was to first collect a significant set of natural goethite samples, characterize them (IR, XRF, N_2 -BET, XRD), and compare the analytical results considering the chemical variability with yet published data. Apart from investigating yet published contradictory results (see Table 1) the present study is also thought to provide comprehensive data on a significant set of natural crystallised goethites.

2 Materials and methods

Twenty eight natural goethite samples which apparently did not contain admixtures were collected. Samples were taken from the BGR mineral collection (both bought from mineral traders and collected in the frame of projects) and BGR reference material sample base (“S-samples”). The samples were crushed and ground using a rotating disc mill and analyzed with respect to the chemical composition by XRF (PANalytical Zetium spectrometer; ALMELO, The Netherlands). Samples were prepared by mixing with a flux material (lithium metaborate Spectroflux, Flux No. 100A, Alfa Aesar) and melting into glass beads. The beads were analyzed by wavelength-dispersive XRF. To determine loss on ignition (LOI), 1000 mg of sample material were heated to $1030\text{ }^\circ\text{C}$ for 10 min including a ramp at $700\text{ }^\circ\text{C}$.

For XRD Rietveld analysis the crushed samples were ground by a McCrone mill using ethanol. XRD patterns were recorded using a PANalytical X’Pert PRO MPD Θ - Θ diffractometer (Co- K_α radiation generated at 40 kV and 40 mA), equipped with a variable divergence slit (20 mm irradiated length), primary and secondary soller, diffracted beam monochromator, point detector, and a sample changer (sample diameter 28 mm). The samples were investigated from 1° to $75^\circ 2\Theta$ with a step size of $0.03^\circ 2\Theta$ and a measuring time of 12 s per step. For specimen preparation the back loading technique was used. Rietveld refinement

of the experimental XRD data was conducted using the software Profex/BGMN (Kustova et al. 1992; Bergmann et al. 1998). This software uses a fundamental parameter approach. This allows to differentiate the instrument depending peak broadening and the sample depending peak broadening. As a consequence refinement of crystallite sizes was possible.

The structural model used for the Rietveld refinements of the goethites was based on (Harrison et al. 1975). The lattice parameters *a*, *b* and *c* were refined within a reasonable range of $\pm 1\%$. No refinement reached these constraints. The fundamental parameter approach of the Rietveld software allows the refinement of anisotropic crystallite size. No additional lattice strain was refined. No attempt was made to refine the positions of the atoms in the unit cell. Only the substitution of Fe (occFe) by Al (occAl) was refined as $\text{occFe} = 1 - \text{occAl}$ starting with $\text{occAl} = 0$ between zero and one.

All other minerals were refined using the standard models of the Rietveld software. In some cases small proportions of admixtures like e.g. kaolinite, as indicated by IR, could not be detected by XRD and therefore were ignored. These admixtures are declared in Table 2.

For measuring mid infrared (MIR) spectra the KBr pellet technique (1 mg sample/200 mg KBr) was applied. Spectra were collected on a Thermo Nicolet Nexus FTIR spectrometer (MIR beam splitter: KBr, detector DTGS TEC). The resolution was adjusted to 2 cm^{-1} . Measurements were conducted before and after drying of the pellets at $150 \text{ }^\circ\text{C}$ in a vacuum oven for 24 h. The OH-bands of unheated pellets are dominated by adsorbed water masking the structural OH bands which are more specific for minerals. Therefore, the spectra of heated pellets were preferred for characterization of the samples. Drying at $150 \text{ }^\circ\text{C}$ is not believed to affect the goethite structure. The IR spectrometer was built by Nicolet Instruments, Madison, Verona Road, Wisconsin, USA. The band maxima were determined based on the maximum value of absorption rather than a gravimetric center or similar algorithms to determine peak maxima.

SSA was determined by N_2 adsorption using a five point BET method. Measurements were performed by a Micromeritics (Norcross/Georgia) Gemini III 2375 surface area analyzer with ca. 300 mg weight. Powders were degassed at $150 \text{ }^\circ\text{C}$ for 24 h under vacuum. Heating is performed in order to “clean” the surface, i.e. remove adsorbed gas and water molecules. Sites which are blocked before starting N_2 adsorption will not be recognized. Different “cleaning” procedures are used (varying *T* and *t* including or excluding low pressure) which slightly affects the values. Comparing different samples it is, therefore, important to keep the sample preparation constant.

3 Results and discussion

3.1 Basic characterisation

The chemical and mineralogical composition of the samples quantitatively investigated by XRD and qualitatively by IR is given in Table 2.

The Al_2O_3 content of the samples ranged from 0 to 8.5 mass% but the high Al-values of samples S038 and S342 resulted from admixtures such as kaolinite or feldspar and hence could not be attributed to structural Al of the goethites. The Al_2O_3 content of the pure goethites for which it could be attributed to structural Al ranged from 0 to 2 mass% which is expectedly lower compared to the synthetic goethites prepared by (Ruan et al. 2002). Also the Al-content of soil or laterite goethites can be significantly higher but these samples, as discussed above, are rarely pure goethites and hence effects of admixtures can hardly be distinguished. Even the macroscopically pure goethites used in the present study showed a couple of admixtures. For 15 samples of the present study a goethite content of ≥ 97 mass% was found. These samples are particularly valuable for studying structural and spectral features. Rietveld refinement indicated the presence of substantial amounts of hematite with goethite in some samples which can be either a mixture of separate phases or the existence of hematite domains within in the structure (e.g. caused by partial dehydroxylation).

The trace elemental concentrations mostly were not highly correlated with each other. A fairly good correlation, however, was observed for Ni and Co which both were only weakly correlated with Cr and Al. No correlation was found between Pb and Zn but a weak one was found for Ba and W. The two samples from Guinea showed the highest Cr-contents ranging from 0.5 to 1.3 mass%. Three samples showed As-contents above 0.1 mass% and three others showed Cu-contents above 0.1 mass%. The latter three also contained high amounts of Pb but other samples in turn showed high Pb-contents and low Cu- contents. Two samples showed Zn-contents in the %-range, other trace elements were less relevant.

3.2 IR spectroscopy

The spectra of the 15 most pure samples (all > 97 mass% goethite) are shown in Fig. 1 and the distributions of the positions of the main goethite bands of all samples are shown in Fig. 2.

The OH-stretching vibration was reported to range from 3100 to 3230 cm^{-1} . The 28 different goethites showed a broad distribution of band positions between 3120 and 3160 cm^{-1} . The average value of all samples is 3143 cm^{-1}

Table 2 Mineralogical and chemical composition of the samples (selected elements) and BET-value. As-values have to be treated with care because part of the As may be evaporated upon ignition

Sample No	Location	Country	XRD Rietveld																		
			Goethite	Hematite	Quartz	Feldspar	Mica	Calcite	Anatase	Anhy./gyp	Lepidocrocite	Smectite									
S 019	Conakry	Guinea	100																		
S 034	Conakry	Guinea	95	5																	
S 038	Vogelsberg	Germany	64	1	< 1						2										32
S 092	Aachen	Germany	96	3	1																
S 178	Diepenlinchen	Germany	100																		
S 179	Kasei Mine	North Korea	100																		
S 249	?	Morocco	83	17																	
S 313	Benalmadena	Spain	100																		
S 337	Sasikmine, Pamir	Pamir	99																		1
S 343	Grube Wolf bei Herdorf	Germany	100																		
S 352	Oberbach, Rhön	Germany	89	11	< 1																
S 374	Clara Mine	Germany	100																		
S 380	Clara Mine	Germany	99	1																	
S 497	Paliz, Palla dil Tgom, Val Blaau	Switzerlnd	99	1																	
S 533	Grube Bollenbach, Herdorf	Germany	100																		
S 534	Clara Mine	Germany	100																		
S 535	Irkuskan Mine, Bakal deposit	Russia	100																		
S 314	Benalmadena	Spain	91	5	1					3											
S 335	RioTinto	Spain	77	23																	
S 340	Weißer Wüste	Egypt	97		< 1																3
S 344	Monument Park, Pretoria	Sout Africa	81	19																	
S 353	Tharsis	Spain	71	29																	
S 355	Waldsascu? Oberpfalz	Germany	70	30																	
S 315	Irisada, Tharsis	Spain	52	48																	
S 342	Caldes de Malavella, Girona	Spain	86		3	4	6														
S 532	Lautenthal, Lindthal, Friederike	Germany	94		6																
S 537	Loßberg-West, Schwarzwald	Germany	99		1																
S 538	Innerstetalsperre, Friederike	Germany	97		3																

Table 2 continued

Sample No	IR						
	Gibbsite	Kaolinite	Quartz	Hematite	Calcite	Anhydrite	
S 019							
S 034							
S 038		+					
S 092							
S 178							
S 179							
S 249							
S 313							
S 337							
S 343							
S 352							
S 374							
S 380							
S 497							
S 533							
S 534							
S 535					+		
S 314							
S 335		?					
S 340						?	
S 344							
S 353		+					
S 355		+	?				
S 315		+					
S 342		+	?				
S 532							
S 537			?				
S 538			?				

Table 2 continued

Sample No	Location	Country	XRF										BET				
			SiO ₂	TiO ₂	Al ₂ O ₃	Fe ₂ O ₃	MnO [mass%]	LOI [mass %]	As [ppm]	Co [ppm]	Cr [ppm]	Cu [ppm]	Mo [ppm]	Ni [ppm]	Pb [ppm]	Zn [ppm]	[m ² /g]
S 019	Conakry	Guinea	2.2	0.1	1.1	79	1.7	13	20	496	13,739	39	0	5274	535	598	54
S 034	Conakry	Guinea	2.9	0.1	1.6	82	0	11	4	183	5713	95	0	2646	0	317	11
S 038	Vogelsberg	Germany	1.5	1.6	8.5	55	0.2	16	0	124	687	56	0	946	11	335	78
S 092	Aachen	Germany	3.7	0	0.1	78	0.7	15	43	20	11	<10	43	20	1323	11,111	42
S 178	Diepenlinchen	Germany	5.4	0	0.6	77	0.4	14	20	16	6	<6	0	36	626	10,490	n.d
S 179	Kasei Mine	North Korea	2.1	0	0.1	84	0.4	13	6	17	0	<7	0	0	0	38	15
S 249	?	Morocco	1.6	0	0.2	92	0.3	5.8	104	0	0	26	0	20	457	72	1
S 313	Benalmadena	Spain	2.2	0	0.8	84	0	12	3096	51	19	384	643	60	0	279	46
S 337	Sasikmine, Pamir	Pamir	2.3	0	0.2	82	1.6	13	84	0	0	305	0	0	11	58	11
S 343	Grube Wolf bei Herdorf	Germany	2.2	0	0.3	85	0.3	12	66	22	0	575	0	55	468	734	7
S 352	Oberbach, Rhön	Germany	5.1	0	0.2	83	0.4	11	69	25	0	26	0	22	42	47	25
S 374	Clara Mine	Germany	4.7	0	0.5	84	0.2	10	63	35	0	237	0	97	0	137	8
S 380	Clara Mine	Germany	4.7	0	0.2	80	0.7	13	224	0	0	209	0	0	0	77	22
S 497	Paliz, Palla dil Tgom, Val Blaua	Switzerland	4.3	0	0.7	76	1.5	17	335	36	0	42	61	86	50	378	85
S 533	Grube Bollenbach, Herdorf	Germany	2.6	0	0	84	0.2	12	241	59	0	0	0	101	0	1315	14
S 534	Clara Mine	Germany	4	0	0.2	81	1.8	12	14	0	0	125	0	0	0	43	22
S 535	Irkuskan Mine, Bakal deposit	Russia	2.2	0	0.1	84	0.3	13	0	0	0	0	0	0	0	38	12
S 314	Benalmadena	Spain	3.7	0	0.4	77	0	15	4282	32	0	519	1849	76	0	386	36
S 335	RioTinto	Spain	0.9	0	0.6	86	0	12	384	14	0	466	0	0	1608	353	20
S 340	Weißer Wüste	Egypt	3.1	0	0.4	78	0	14	61	27	114	66	9	228	21	4095	7
S 344	Monument Park, Pretoria	Sout Africa	2.7	0	0.4	84	0	11	2395	14	277	59	0	31	10	57	14
S 353	Tharsis	Spain	2.4	0	1.6	83	0	12	652	11	0	1038	0	0	10,380	280	28
S 355	Waldsassen? Oberpfalz	Germany	1.8	0	1.9	84	0	12	45	0	0	2726	0	0	680	456	16
S 315	Irisada, Tharsis	Spain	2.6	0	1.7	84	0	9.7	816	13	16	1296	0	7	12,040	138	27

Table 2 continued

Sample No	Location	Country	XRF										BET				
			SiO ₂	TiO ₂	Al ₂ O ₃	Fe ₂ O ₃	MnO [mass%]	LOI [mass %]	As [ppm]	Co [ppm]	Cr [ppm]	Cu [ppm]	Mo [ppm]	Ni [ppm]	Pb [ppm]	Zn [ppm]	[m ² /g]
S 342	Caldes de Malavella, Girona	Spain	14	0.1	3.9	66	0.6	13	55	41	16	56	0	248	0	335	11
S 532	Lautenthal, Lindthal, Friederike	Germany	9.1	0	0.1	78	1.2	12	0	27	0	0	0	97	0	67	17
S 537	Loffberg-West, Schwarzwald	Germany	5.7	0	0	79	0.7	14	0	0	0	0	0	0	28	20	36
S 538	Innerstetsperre, Friederike	Germany	6.7	0	0	80	0.4	12	0	44	0	119	0	110	0	45	15

which corresponds well with the sample of highest crystallinity reported by Cambier 1986b) and with the upper limit of the range reported by (Marel and Beutelspacher 1976). The band shape of all samples is similar (Fig. 1 left). Differences were observed at about 3400 cm⁻¹ where a few samples exhibited a shoulder (S034, S179, S374). This shoulder, which is significantly reduced upon drying at 150 °C in a vacuum oven, is supposed to result from water strongly bound to micropores (either of goethite or even caused by small ferrihydrite admixtures although ferrihydrite is rarely found in natural goethites). Based on a set of synthetic samples (Houben and Kaufhold 2011) showed that the ratio of the 3410–3140 cm⁻¹ bands in a ferrihydrite-goethite series correlated well with the ferrihydrite content and the specific surface area, respectively. Consequently, this shoulder could correspond to ferrihydrite as admixture or even as domains within the goethite structure. However, samples which showed this shoulder did not show higher surface area values (which corresponds to microporosity).

The bands between 1000 and 2000 cm⁻¹ are weak and hence rarely discussed in literature. Moreover, they are known to strongly depend on drying and sample preparation (Morterra et al. 1984). Goethite, as an anhydrous oxyhydroxide, should not show any bands in this region resulting from lattice vibrations. These bands more likely represent water bound to the surface or micropores. In the spectra recorded before drying at 150 °C in a vacuum oven the OH—bending mode of molecular water (ca. 1630 cm⁻¹) dominated in this range and expectedly decreased after drying. The remaining intensity around 1640 cm⁻¹, therefore, was attributed to a combination mode of the bands around 900–800 cm⁻¹ (Schulze 1984) rather than molecular water. The least intense band of most pure samples in this region was centered at about 1760 cm⁻¹. Morterra et al. (1984) attributed this band to an overtone of the band near 900 cm⁻¹. Its band position, therefore, depends on the band position of the band near 900 cm⁻¹. Interestingly the most pronounced intensity in the range from 1000 to 2000 cm⁻¹ was found at about 1510 cm⁻¹. This band is hardly described in literature and hence could not be assigned unambiguously. Morterra et al. (Hazemann et al. 1992) (Fig. 3) showed a spectrum in which this band appeared after 200 °C heat treatment but it was not discussed further. Interestingly, this band was not observed by these authors after using a different sample preparing technique (film) despite heating to 200 °C. In the present study this band was observed for almost all pure samples, except for S034 and S374 and only weak intensity was found for S533 and S343. Notably the band was only observed in the spectra collected after drying at 150 °C in a vacuum oven (standard routine in the present study) which means that structural changes may

have occurred in some samples which led to the appearance of this band. No other significant band shifts or intensity ratio changes were observed upon drying which suggests that this band is not a combination of e.g. the 900 and 630 cm^{-1} bands, because such a band would have been observable before drying. Interestingly this band is also observed for some hematites but not for all. Based on the present sample set it was not possible to unambiguously explain this band. The bands between 1000 and 2000 cm^{-1} are not investigated further because of their weak intensity and because as combination or overtone they do not provide more information compared with the primary vibrations.

The in-plane OH deformation band around 900 cm^{-1} was mostly located around 894 cm^{-1} . The out of plane vibration was around 797 cm^{-1} with only few exceptions showing larger band positions. Both average values are in good agreement with the ranges summarized in Table 1.

The Fe–O stretching band showed a sharp distribution around 610 cm^{-1} which is lower compared to most of the reported values (Table 1). The Fe–OH stretching bands were found at 450 and 410 cm^{-1} which corresponds well to most of the published values. The 450 cm^{-1} band positions showed a sharp distribution whereas the 410 cm^{-1} maxima were more variable.

Spectral differences generally do not only concern band positions but also relative intensities. The relative intensities of the bands $> 500 \text{ cm}^{-1}$, including the intensity of the shoulder at 680 cm^{-1} compared to the intensity of the 610 cm^{-1} band, were similar. The ratio of the 450 and 410 cm^{-1} bands, however, were significantly different. Most samples showed a dominating 410 cm^{-1} band and a shoulder at 450 cm^{-1} but some samples showed more or less similar intensity (S019, S034, S313, S537). Sample

S374 even showed a more intense 450 cm^{-1} band resulting in a shoulder at 410 cm^{-1} . The main bands of hematite are at 550 and 460 cm^{-1} . The presence of some hematite would, therefore, explain higher intensity at around 450 cm^{-1} but the even more intense band at 550 cm^{-1} should be observable which was not the case for any of the pure samples. The varying intensity ratio, therefore, cannot be explained by hematite or hematitic domains. However, a correlation of both bands with SSA was observed which is discussed later.

3.3 Geochemical effect on band position

The band positions were compared with the trace elemental composition and the resulting regression coefficients are listed in Table 3. Positive relations (increasing x corresponds to increasing y) were marked by “+” and negative ones (increasing x corresponds to decreasing y) by “-”. Regression coefficients which apparently result from few particularly high values are given in brackets.

Ruan et al. (2002) reported increasing band positions of the OH-stretching band around 3140 cm^{-1} with increasing Al-content. This relation could not be confirmed in the present study possibly because of much lower Al-contents of the goethites. Instead a slight dependency of the band position on the LOI value was found (Fig. 4a). At the same time a correlation of the band position and SSA was found. Both can probably be explained by water bound to micropores which would provide intensity around 3400 cm^{-1} and hence slightly shift the maximum and at the same time increase the LOI. This data suggests that the increase of the band position with increasing Al-content reported by Ruan et al. (2002) could be explained by different microporosity (or crystallinity) of the different

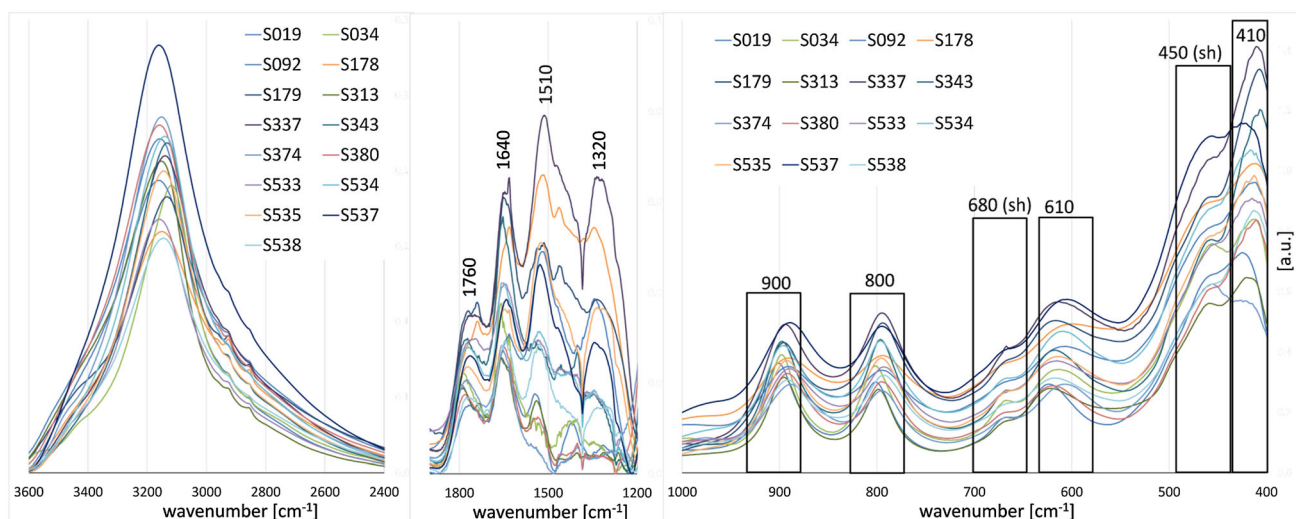


Fig. 1 MIR spectra of 15 natural goethite samples (purity $> 97\%$)

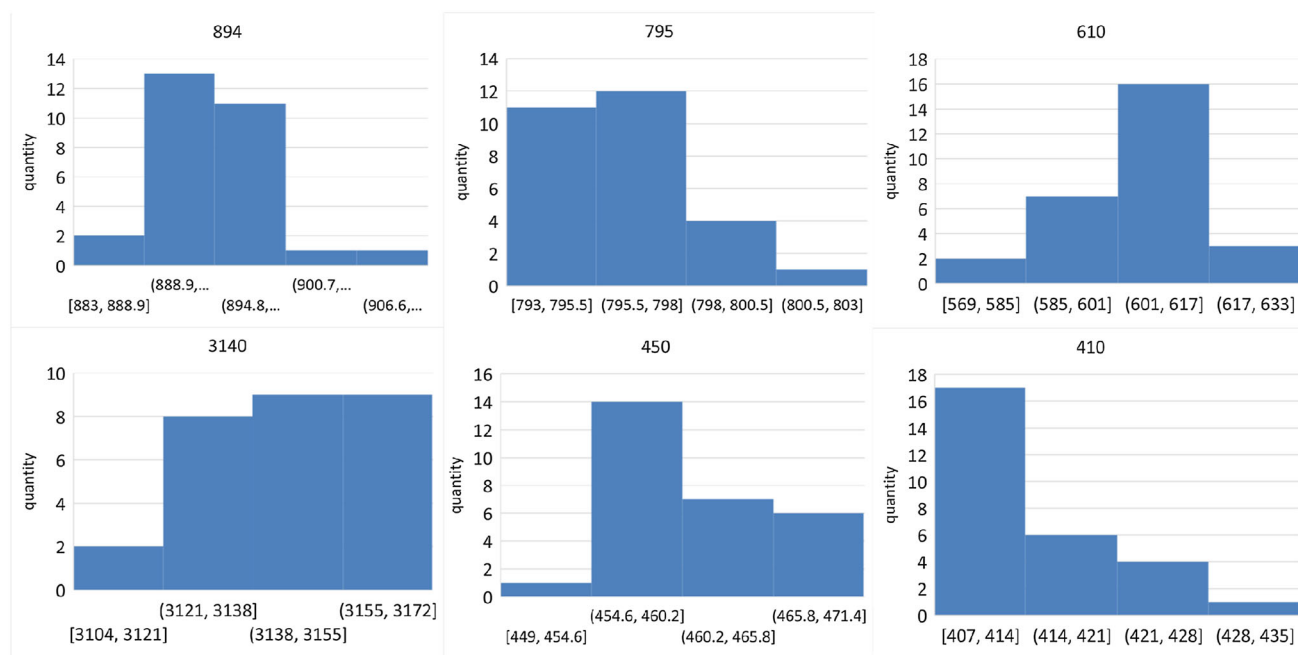


Fig. 2 Statistical analysis of the band positions of the most important bands of all samples. Unit y-axis: number of samples with band positions in the respective range

synthetic samples which then would indicate increasing microporosity of the synthetic samples with increasing Al-content.

The OH-bending band position (1645 cm^{-1}) showed a negative correlation with the LOI (Fig. 4b) which cannot be explained yet. The correlation of this band position with the Fe-content suggests that it is affected by the purity of the sample (presence of trace phases).

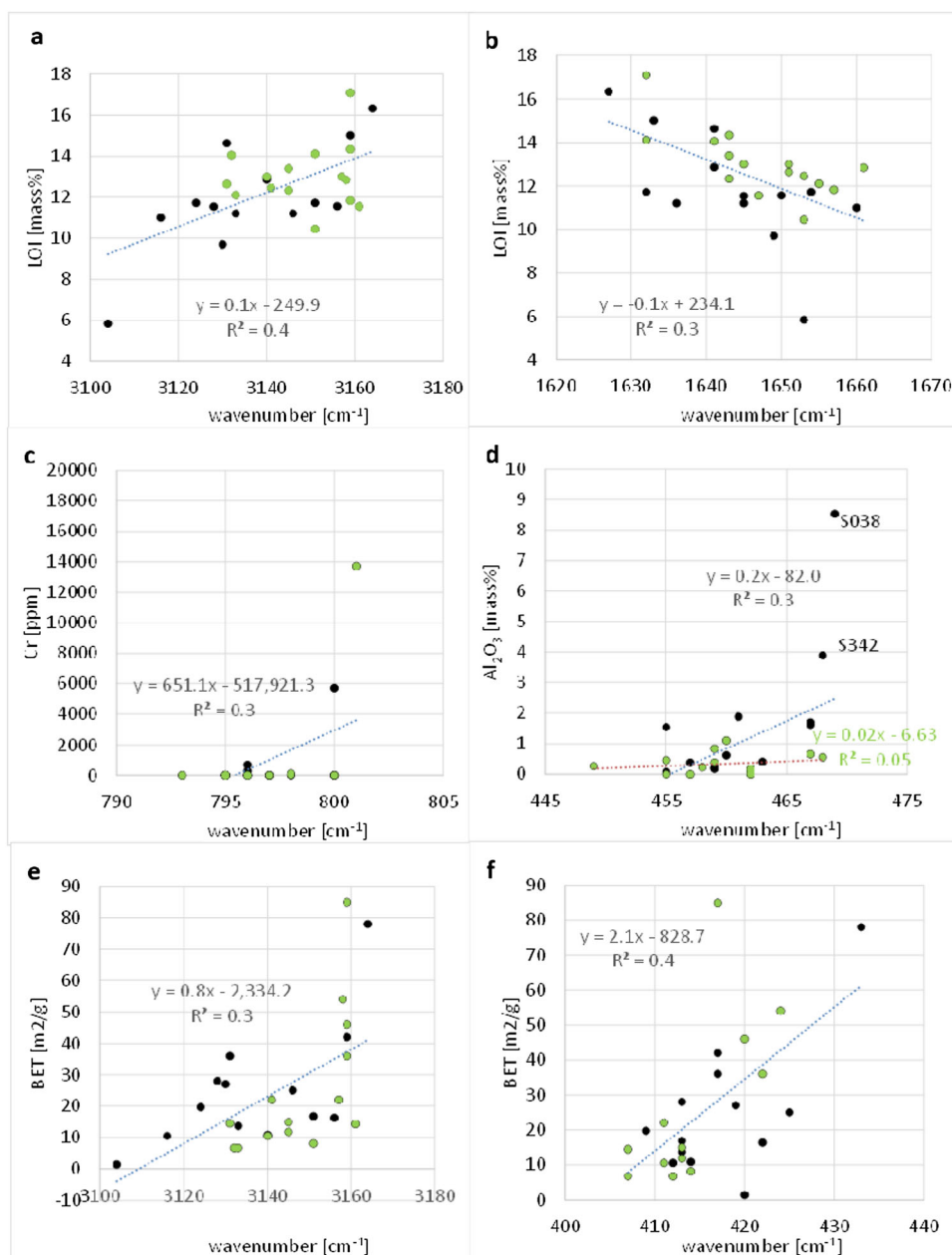
Significant effects of the Al-content on the band positions $< 1000\text{ cm}^{-1}$ were reported by Ruan et al. (2002) and Blanch et al. (2008) (Table 1). Data presented in the present study confirms most of these trends but not all of them. The 900 cm^{-1} band increases as Al increases which is in agreement with Ruan et al. (2002). In addition to Al, Cr has a similar effect (Fig. 4c). With increasing Cr-content a shift of the band to higher wave numbers was observed. The same holds true for the 800 cm^{-1} band which was also observed before (Table 1). No trend was observed for the 610 cm^{-1} band in the present study and different trends were reported by Ruan et al. (2002) and Blanch et al. (2008). This result suggests that the opposing trends published by these authors did not result from varying Al-contents but from other parameters such as crystallinity (as suggested by (Sato et al. 1969)) which were probably indirectly affected by preparing synthetic samples with different Al-content. On the other hand, the positive Cr-correlation is based on two samples only (S109). This sample contains 2.0 mass% MnO (XRF) that may also be related to Cr in an unknown phase (compare

(Singh et al. 2002)) who point out that “transition metals such as Cr, Mn and Ni may sorb onto goethite by forming surface precipitates, surface complexes or by replacing Fe^{3+} in the goethite structure.”. In the sample set used in the present study the band position distribution of the 610 cm^{-1} band was sharper compared to the others and no correlations with any other parameter were observed which indicates that this band position is less affected by chemical variations compared to the others. Also for the 450 cm^{-1} band/shoulder different trends were reported (Table 1). The sample set of the present study apparently confirmed the positive relation of the 450 cm^{-1} band position and the Al-content published by (Ruan et al. 2002) (Fig. 4d) but the trend mainly results from two samples (S038, S342) containing accessories such as smectite and feldspar. The 450 cm^{-1} can be affected by accessories such as Al-hydroxides and Al-silicates and hence must be treated with care. Data presented in Fig. 4d neither confirms Ruan et al. (2002) nor Blanch et al. (2008) because no clear trend was observed.

3.4 XRD

The parameters describing the structural features of the goethites derived from XRD are summarized in Table 4. Rietveld refinement generally allows to refine a huge set of different parameters. Commonly as many as possible of these parameters are fixed in order to increase the significance of the results. In order to find out which parameters

Fig. 3 Correlations of XRD Rietveld parameters with IR spectroscopic data. Red lines in c and d represent specific surface areas (SSA) calculated based on the refined crystallite sizes and on assuming rectangular particles with a density of 4.27 g/cm^3 . The estimated standard deviation of the crystallite size was $< 1 \text{ nm}$, the dimension of the symbols hence represent the expected error



can be reasonably fixed and which can be used to better describe the XRD results (and hence improve the quality of the Rietveld refinement), different refinements with different sets of parameters are used and the resulting “goodness of fits” are used to assess the quality of the different refinements. As an example, the occupation of lattice positions by Al was included in the Rietveld refinement but the results did not result in reasonable values (which, e.g. could be compared with the chemical analysis). This may be different in case of samples with higher degree of isomorphic substitution. Linear relationships of the lattice parameters to the substitution of Fe by

Al, as described in Schulze (1984), confirm that the samples contain nearly no structural Al in the goethites.

Variation of the lengths of the axes was small and therefore no significant relation was found with other XRD or IR derived parameters. These variations could possibly be explained by lattice stress but this parameter could not reasonably be refined by Rietveld refinement. The best but still weak trend was observed for the length of the b-axis and the band position of the 3140 cm^{-1} band but this trend mostly results from one sample only (S038) and hence is not considered to be significant (not shown). Notably, sample S374 contains two different goethites (with slightly different peak positions) for which no reasonable data

Table 3 Regression coefficients of the band position and the trace elemental composition

	3140 [cm ⁻¹]	1645 [cm ⁻¹]	900 [cm ⁻¹]	800 [cm ⁻¹]	610 [cm ⁻¹]	450 [cm ⁻¹]	410 [cm ⁻¹]
Si	0.1	0.2	0	0.1	0	0	0.1
Ti	0	0.2	(0.3 +)	0.1	0	0.2	(0.3 +)
Al	0	0.2	(0.3 +)	0	0	(0.3 +)	(0.3 +)
Fe	0.1	0.4 +	0.1	0	0	0	0
Mn	0.1	0	0	0	0	0	0
Mg	0	0.1	0	0	0	0	0
P	0.1	0.1	0	0	0	0.1	0
LOI	0.4 +	0.3 -	0	0	0	0.1	0
As	0	0	0.1	0	0	0	0
Ba	0	0	0	0	0	0	0
Co	0	0.1	0.1	0.1	0.1	0	0.1
Cr	0	0	(0.2 +)	0.3 +	0.1	0.2	0
Cu	0	0.1	0	0	0.1	0	0
Mo	0	0	0.1	0	0	0	0
Ni	0	0.1	0.1	0.1	0.1	0	0.1
Pb	0	0	0	0	0	0.1	0
W	0	0	0	0	0	0	0
Zn	0	0.1	0	0	0	0	0
BET	0.3 +	0.2	0	0.1	0	0.3 +	0.4 +

+ positive correl. (+ WN = + content), - = negative corr., brackets = correl. based on few samples only

Bold: most significant regressions

could be obtained from Rietveld refinement. The fact that quite constant values for the lengths of the axes were found does not indicate that this is necessarily true but it does indicate that other parameters, i.e. crystallite size, determine the variability of the XRD patterns.

Weak trends were observed for the crystallite size with band positions of the 450 and 3140 cm⁻¹ bands (Fig. 3a, b, e, f). The crystallite size, resulting from Rietveld refinement, representing the dimension of the coherent scattering domain (not the particle size), also could be related to the specific surface area (SSA). Particularly the lengths of the crystallites in a and c direction (Fig. 3c, d) showed a good correlation with SSA. The SSA of soil and synthetic goethites often results from microporosity (including ferrihydrite admixtures, Houben and Kaufhold (2011)). The data shown in Fig. 3c, d, however, suggests that the SSA is actually determined by the crystallite size. The red curves in Fig. 3c, d represent SSA values calculated based on the crystallite sizes assuming a density of 4.27 g cm⁻³ and cubic shape of the (theoretical) particles. The good correlation of crystallite size and SSA and the similarity with calculated values (red curves) indicates that the Rietveld refinement yielded reasonable values. Interestingly lower SSA values were measured compared to the calculated SSA. This indicates that microporosity which in the ferrihydrite-goethite series determines SSA is low in these

samples because microporosity would increase the SSA. At the same time the lower measured values indicate that N₂ could not enter between all crystallites (defined as the coherent scattering units). The fact that lower values were measured compared to the calculated ones, therefore, can be explained by the existence of particles consisting of several crystallites not allowing nitrogen to enter.

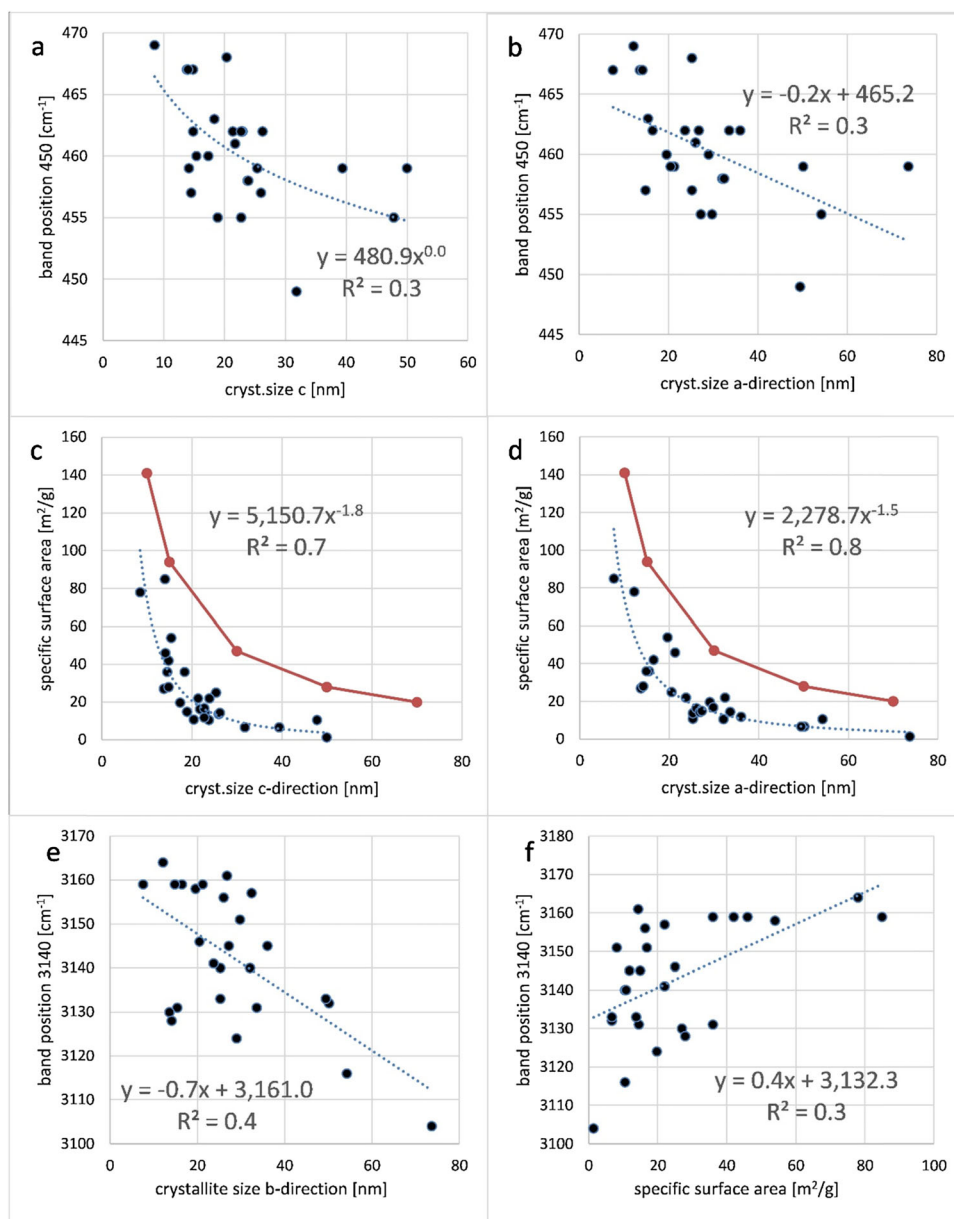
Sato et al. (1969) concluded that the band at 610 cm⁻¹ is particularly useful to study the crystallinity of the goethite but neither a correlation with SSA nor with crystallographic parameters of this band was found.

4 Conclusion

The samples investigated in the present study did not cover the entire range of chemical compositions of natural goethites but the advantage of these samples was that they did not contain accessories affecting either XRD or IR results. Accordingly yet published ambiguous results could be explained based on the findings of the present study.

Also Rietveld refinement was optimized based on comparing the different results. Commonly Rietveld results derived from refinements using different parameters are assessed based on the “goodness of fit”. In the present study a fairly good correlation of the crystallite size and the

Fig. 4 Selected correlations of band positions geochemical parameters. Samples marked in green contain > 97 mass% goethite. The regression coefficient is based on all samples



specific surface area was found. This is remarkable because N_2 -adsorption—being completely independent from XRD—indicated the significance of the refined crystallite sizes and hence proved that it is important to include them to improve Rietveld refinement of (crystallised) goethites. The good correlation of SSA and refined crystallite sizes proves that (i) the refinement yielded reasonable and significant values and (ii) that the content of possibly existing microporous admixtures such as ferrihydrite or amorphous Fe-oxyhydroxides was low and hence could not affect the trends identified in the present study.

Contradictory results were published for the effect of the Al-content on the position of the band at 450 cm^{-1} , (Blanch et al. 2008): decrease; (Ruan et al. 2002): increase

with increasing Al. The goethites investigated in the present study neither confirmed the trend published by (Ruan et al. 2002) nor by (Blanch et al. 2008) which could result from the limited chemical variability of the samples. However, a good correlation of the 450 cm^{-1} band with the crystallite size was found. The ambiguous results published by (Ruan et al. 2002) and (Blanch et al. 2008) hence can be explained by differently varying crystallite sizes in their sample sets.

The band position of the band at 610 cm^{-1} was reported to depend on the Al-content, (Blanch et al. 2008): increase; (Ruan et al. 2002): decrease, and (Sato et al. 1969) reported that this band can be used to assess the crystallinity of the goethites. In the present study this band proved to be least

Table 4 Crystallographic and morphological data derived from XRD Rietveld refinement

	Lattice parameter			Cryst. size		
	a-axis [nm]	b-axis [nm]	c-axis [nm]	c-direction [nm]	a-direction [nm]	b-direction [nm]
S 019	0.996	0.302	0.460	15.4	19.6	26.0
S 034	0.996	0.302	0.460	47.8	54.2	41.6
S 038	0.991	0.300	0.459	8.5	12.1	15.7
S 092	0.996	0.302	0.461	14.8	16.5	23.7
S 179	0.996	0.302	0.461	22.9	33.6	33.6
S 249	0.995	0.302	0.460	50.0	73.7	72.1
S 313	0.996	0.302	0.461	14.1	21.3	39.1
S 314	0.998	0.303	0.462	18.3	15.4	25.9
S 315	0.999	0.303	0.463	13.8	13.6	21.6
S 335	0.997	0.303	0.462	17.3	29.0	39.0
S 337	0.995	0.302	0.461	23.8	32.1	30.0
S 340	0.996	0.302	0.461	39.4	50.2	57.6
S 342	0.996	0.302	0.462	20.4	25.3	24.9
S 343	0.995	0.302	0.461	31.8	49.5	44.0
S 344	0.996	0.302	0.461	26.0	25.3	24.6
S 352	0.995	0.302	0.461	25.4	20.5	22.2
S 353	0.997	0.302	0.462	14.8	14.1	28.2
S 355	0.995	0.302	0.461	21.8	26.0	30.9
S 374	0.994	0.303	0.461	118.0	98.0	37.6
S 380	0.996	0.302	0.462	23.9	32.4	38.1
S 497	1.001	0.303	0.463	14.0	7.6	13.2
S 532	0.996	0.302	0.461	22.7	29.8	30.1
S 533	0.995	0.302	0.461	26.2	26.8	28.9
S 534	0.996	0.302	0.461	21.4	23.7	30.1
S 535	0.995	0.303	0.461	22.7	36.0	32.8
S 537	0.999	0.303	0.463	14.5	14.9	22.4
S 538	0.996	0.302	0.461	18.9	27.2	29.5

variable, neither depending on chemical composition nor on structural parameters (including specific surface area) which can possibly be explained by the relatively low degree of Al substitution of the samples compared with other synthetic and soil goethites studied before.

The OH stretching band near 3100 cm^{-1} showed relations with the LOI, specific surface area, and the crystallite size. The relations of the band position with LOI and surface area could be explained by the amount of micropores which would affect the specific surface area and provide some IR intensity at 3400 cm^{-1} hence causing a slight shift towards higher wavenumbers. This explanation, however, remains unlikely because SSA was determined by crystallite size and the samples were low in microporosity. The OH stretching band is related to the crystallite size although the reason for this relation could not be identified.

The results of the present study indicate that using synthetic sample sets bears the problem that more than one

parameter might show systematic differences (e.g. crystallite size in a set of chemically varied goethites). The paper, therefore, provides IR reference data based on a set of natural well crystallised goethites.

Acknowledgements The authors like to acknowledge Frank Korte for providing the chemical analyses.

Author contributions Conceptualization, writing, and visualization, SK; methodology and investigation, MH, NG; data curation, writing, review, editing, and supervision, KU and RD.

Funding Open Access funding enabled and organized by Projekt DEAL. This research received no external funding.

Declarations

Conflicts of interest The authors declare no conflict of interest.

Ethical approval All authors have approved the manuscript and agree with its submission.

Informed consent We confirm that neither the manuscript nor any parts of its content are currently under consideration or published in another journal.

Open Access This article is licensed under a Creative Commons Attribution 4.0 International License, which permits use, sharing, adaptation, distribution and reproduction in any medium or format, as long as you give appropriate credit to the original author(s) and the source, provide a link to the Creative Commons licence, and indicate if changes were made. The images or other third party material in this article are included in the article's Creative Commons licence, unless indicated otherwise in a credit line to the material. If material is not included in the article's Creative Commons licence and your intended use is not permitted by statutory regulation or exceeds the permitted use, you will need to obtain permission directly from the copyright holder. To view a copy of this licence, visit <http://creativecommons.org/licenses/by/4.0/>.

References

- Bergmann J, Friedel P, Kleeberg R (1998) BGMN—a new fundamental parameters based Rietveld program for laboratory X-ray sources, its use in quantitative analysis and structure investigations. *CPD Newsl* 20:5–8
- Blanch AJ, Quinton JS, Lenehan CE, Pring A (2008) The crystal chemistry of Al-bearing goethites: an infrared spectroscopic study. *Mineral Mag* 72:1043–1056
- Cambier P (1986a) Infrared study of goethites of varying crystallinity and particles size: I. Interpretation of OH and lattice vibration frequencies. *Clay Miner* 21:191–200
- Cambier P (1986b) Infrared study of goethites of varying crystallinity and particle size: II. Crystallographic and morphological changes in series of synthetic goethites. *Clay Miner* 21:201–210
- Fassbinder J, Stanjek H, Vali H (1990) Occurrence of magnetic bacteria in soil. *Nature* 343:161–163
- Fysch SA, Fredericks PM (1983) Fourier transform infrared studies of aluminous goethites and hematites. *Clays Clay Miner* 31:377–382
- Goldschmidt VM (1926) *Geochemische verteilungsgesetze der elemente*. Skrifter norske videnskaps akad, Oslo (in German)
- Hakeem NA, Basily AB, Sagr N, Moharram MA (1986) Study of the thermal transformation of natural goethite using infrared spectroscopy. *J Mater Sci Lett* 5:4–6
- Harrison RK, Aitkenhead N, Young BR, Dagger PF (1975) Goethite from hindlow derbyshire. *Bull Geol Surv Great Britain* 52:51–54
- Hazemann JL, Manceau A, Saintavirt Ph, Malgrange C (1992) Structure of the $\text{Fe}_{x}\text{Al}_{1-x}\text{OOH}$ Solid Solution I. Evidence by polarized EXAFS for an epitaxial growth of hematite-like clusters in Fe-Diaspore. *Phys Chem Mineral* 19:25–38
- Houben G, Kaufhold S (2011) Multi-method characterization of the ferrihydrite to goethite transformation. *Clay Min-Erals* 46:387–395
- Jónás K, Solymár K (1970) Preparation X-ray, derivatographic and infrared study of aluminium-substituted goethites. *Acta Chimica Acad Sci Hung* 66:338–394
- Krehula S, Musić S (2008) Influence of cobalt ions on the precipitation of goethite in highly alkaline media. *Clay Miner* 43:95–105
- Kustova GN, Burgina EB, Sadykov VA, Poryvaev SG (1992) Vibrational spectroscopic investigation of goethite thermal decomposition products. *Phys Chem Mineral* 18:379–382
- Levard C, Borschneck D, Grauby O, Rose J, Ambrosi JP (2018) Goethite, a tailor-made host for the critical metal scandium: The $\text{FeSc}_{1-x}\text{OOH}$ solid solution. *Geochem Perspect Lett*. <https://doi.org/10.7185/geochemlet.1832>
- Manceau A, Schlegel ML, Musso M, Sole VA, Gauthier C, Petit PE, Trolard F (2000) Crystal chemistry of trace elements in natural and synthetic goethite. *Geochim Cosmochim Acta* 64:3643–3661
- Martin F, Ildelfonse PH, Hazemann J, Mathe P, Noack Y, Grauby O, Beziat D, De Parseval PH (1997) Gallium crystal chemistry in synthetic goethites. *J de Phys IV* 7(C2):C-821–C-822
- Mendelovici E, Yariv Sh, Villalba R (1979) Aluminum-bearing goethite in Venezuelan laterites. *Clays Clay Miner* 27:368–372
- Mikutta R, Kleber M, Torn MS, Jahn R (2006) Stabilization of soil organic matter: association with minerals or chemical recalcitrance? *Biogeochemistry* 77:25–56
- Morterra C, Chiorino A, Borello E (1984) An IR spectroscopic characterization of $\alpha\text{-FeOOH}$ (Goethite). *Mater Chem Phys* 10:119–138
- Norrish K, Taylor M (1961) The isomorphous replacement of iron by aluminium in soil goethites. *J Soil Sci* 12:294–306
- Poggenburg C, Mikutta R, Schippers A, Dohrmann R, Guggenberger G (2018) Impact of natural organic matter coatings on the microbial reduction of iron oxides. *Geochim Cosmochim Acta* 224:223–248
- Rabie MS, Balkees H (1986) Infrared study of $\text{FeO}^*\text{OH} \rightarrow \text{Fe}_2\text{O}_3$ thermal transformation. *Proc Indian Acad Sci* 96:315–320
- Rochester CH, Topham SA (1979) Infrared study of surface hydroxyl groups on goethite. *J Chem Soc Faraday Trans* 75:591–602
- Rose B (2016) *Great myths and legends: the golden age of king midas*. University of Pennsylvania Press, Philadelphia, Penn Museum
- Ruan HD, Frost RL, Klopogge JT, Duong L (2002) Infrared spectroscopy of goethite dehydroxylation. II. Effect of aluminium substitution on the behavior of hydroxyl units. *Spectrochimica Acta Part A* 58:479–491
- Sato K, Sudo T, Kurosawa F, Kammori O (1969) The influence of crystallization on the infrared spectra of α - and γ -ferric oxyhydroxides. *Nippon Kinzoku Gakkaishi. J Japan Inst of Metals* 33:1371–1376
- Scheinost AC, Schulze DG, Schwertmann U (1999) Diffuse reflectance spectra of Al substituted goethite: a ligand field approach. *Clays Clay Miner* 2:156–164
- Schulze DG (1984) The influence of aluminium on iron oxides. VII. Unit-cell dimensions of Al-substituted goethites and estimation of Al from them. *Clays Clay Miner* 32:36–44
- Schulze DG, Schwertmann U (1984) The influence of aluminium on iron oxides. X properties of Al-substituted goethites. *Clay Miner* 19:521–529
- Schulze DG, Schwertmann U (1987) The influence of aluminium on iron oxides. XIII. properties of goethites synthesized in 0.3 M KOH at 25 °C. *Clay Miner* 22:83–92
- Sileo EE, Ramos AY, Magaz GE, Blesa MA (2004) Long-range vs. short-range ordering in synthetic Cr-substituted goethites. *Geochim Cosmochim Acta* 68:3053–3063
- Singh B, Sherman D, Gilkes R, Wells M, Mosselmans J (2002) Incorporation of Cr, Mn and Ni into goethite ($\alpha\text{-FeOOH}$): mechanism from extended X-ray absorption fine structure spectroscopy. *Clay Miner* 37(4):639–649. <https://doi.org/10.1180/000985502374066>
- Thiel R (1963) Zum system $\alpha\text{-FeOOH} - \alpha\text{-AlOOH}$. *Z Anorg Allg Chem* 326:70–78
- Van der Marel HW, Beutelspacher H (1976) *Atlas of infrared spectroscopy of clay minerals and their admixtures*. Elsevier, Amsterdam, p 396
- Verdonck L, Hoste S, Roelandt FF, Van Der Celen GP (1982) Normal coordinate analysis of cr-FeOOH . A molecular approach. *J Mol Struct* 79, 273–279

Wickramarathna S, Chandrajith R, Senaratne A, Paul V, Dash P, Wickramasinghe S, Biggs P (2021) Bacterial influence on the formation of hematite: implications for martian dormant life. *Int*

J Astrobiol 20(4):270–284. <https://doi.org/10.1017/S1473550421000124>